Enhanced Second Harmonic Generation in $Au/Al_2O_3/Au$ absorber

Fenglun Huang, Songang Bai, Qiang Li, Yurui Qu and Qiu Min

State Key Laboratory of Modern Optical Instrumentation, College of Optical Science and Engineering, Zhejiang University, Hangzhou, 310027, China
E-mail: qiangli@zju.edu.cn

Abstract. A kind of metal-insulator-metal (MIM) metamaterial absorber for generating second harmonic signal is investigated. The absorbers exhibit high absorption efficiency at the dip and notably enhance the generated second harmonic signal by a factor of over 30, in contrast to an Au/alumina double-layer without Au disk on the top. This study demonstrates the potential of metamaterial absorber for nonlinear photonics.

1. Introduction

Second harmonic generation (SHG) is a typical nonlinear process, which occurs when the light of suitable wavelength interacts with some nonlinear materials[1,2]. SHG originates from both the surface and the bulk of various nonlinear materials. Unlike other nonlinear processes, the SHG relating to electric-dipole is forbidden in the bulk of a centrosymmetric material, with only negligible electric quadrupole and magnetic dipole predominant [3]. Due to the break of the inversion symmetry at the surface of this kind of material, SHG occurs with a low efficiency[4,5]. The metamaterial can confine light, enhance local field and avoid involvement of phase matching, making surface plasmon resonance from metal nanostructures a good candidate for nonlinear effect [6-9].

Numerous nano-scale metallic structures have been proposed and studied both theoretically and experimentally over the past several years, such as simple geometric hole-type[10-13], metal particles and convex geometry[14-16] structures on isolator substrates, metal film with bull's eye patterns[17], bowtie antennas[18], core-shell on nonlinear crystal substrate[19], special hybrid structures[20] and so on. However, few studies have paid close attention to a special MIM metamaterial absorber structure for exciting SHG with ultrahigh absorption peak.

Here we demonstrate an Au/Al2O3/Au three-layer absorber on silica substrates, as illustrated in Fig. 1a. Figure 1b shows one of its unit cell, where *t*, *d* and *h* denote the thickness of three layers, *r* represents the radius of the gold nanoparticle on the top, and *p* is period of the array.

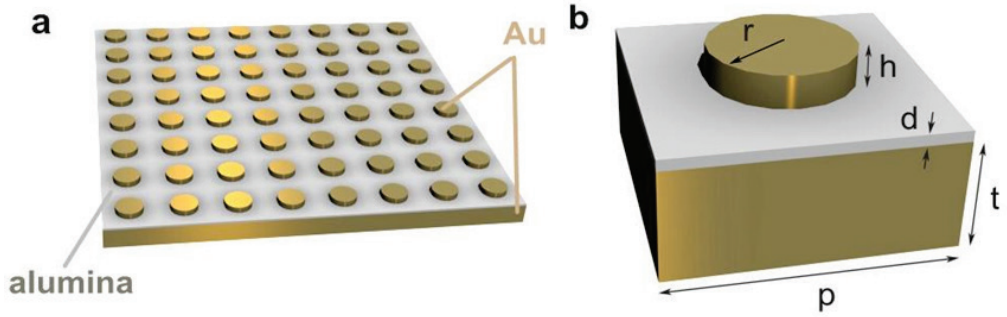

Figure 1. (a) Geometry of MIM three-layer absorber. (b) Unit cell of absorber. Here, *t*, *d*, *h* represent thickness of three layers. *p* is the period of array and *r* denotes radius of Au disk on the top.

2. Numerical simulation

We perform numerical calculations of nonlinear optical properties of the absorbers at normal incidence with finite difference time domain (FDTD) method. By changing structural parameters, influence of different thicknesses, radii and periods on the nonlinearity is studied. Here, thickness of the top Au disk (*h*) is fixed at 30nm, and the thickness of bottom Au (*t*) is set to be thick enough to make sure that no light is transmitted.

The results of the simulation are presented in Fig. 2. At normal incidence, the fundamental resonances at reflection spectra for different radii of Au disks are shown in Fig. 2a. The period *p* and

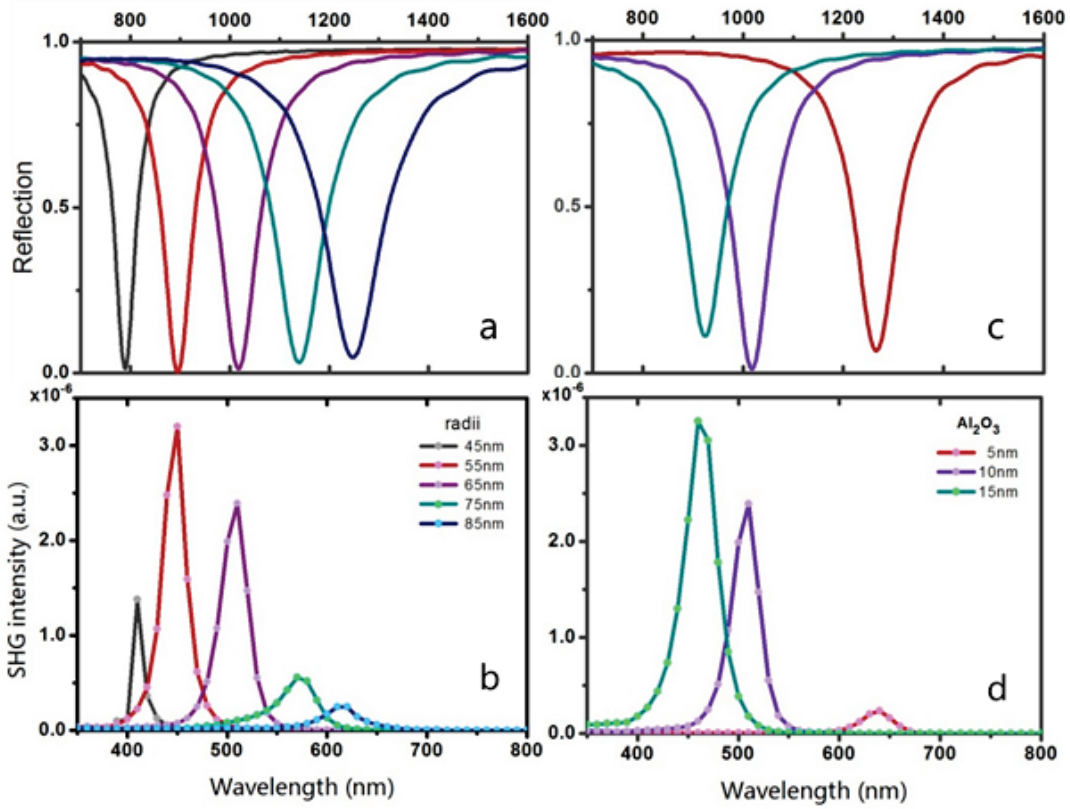

Figure 2. Simulated reflection spectra (a) and SHG intensity spectra (b) of the absorber with different Au disk radii (*r*), where *p*=250nm and *d*=10nm. Simulated reflection spectra (c) and SHG intensity spectra (d) of the absorber with different alumina thickness (*d*), where *p*=250nm and *r*=65nm.

thickness *d* are set to be 250 nm and 10 nm, respectively. At resonant dip, the reflection is close to zero, indicating a high absorption. The resonance shifts to longer wavelength and becomes slightly weaker as the radius of Au disk increases. Figure 2b shows the SHG intensity spectra of absorbers with different radii *r*, where the peaks of each spectrum clearly correspond to the resonance dips. Specifically, the peaks with radii of 55nm and 65nm are much higher than others.

Figure 2c and 2d shows the reflection and SHG intensity spectra of absorbers with different alumina thickness (*d*), where *r*=65nm and *p*=250nm. Resonance shifts towards shorter wavelength as the alumina becomes thicker. SHG peaks are in agreement with the resonance of fundamental wavelength. The maximum SHG is obtained with the thickness of 15nm.

3. Experiment

In our experiment, we fabricate the three-layer MIM structure. The substrate is firstly coated with 100-nm-thickness Au film. Then a 10-nm-thickness alumina is evaporated. After that, Au disks with different radii (with a period of 250nm) are patterned by electron-beam lithography. Figure 3a shows the SEM image of a representative absorber with the radius of Au disk at 65nm. The laser pulse for SHG is generated by a Mira HP-D femtosecond Ti:Sapphire oscillator, successively tuned by a Mira OPO. The power arriving at the sample is attenuated down to 28mW. The SHG signal is collected and measured by a PI TriVista spectrometer in the reflection direction.

Figure 3b shows the measured and simulated reflection spectra of the sample with *r*=65nm. The measured spectrum has a resonant reflection of 30% around 1000nm, while the simulation indicates nearly no reflection at resonance. We experimentally measure the SHG signals reflected by the sample with the incident light near 1000nm where the resonance occurs. The measured and simulated results have been displayed in Fig. 4. The measured SHG signals (dark cyan) agrees well with the simulation except that it is shifted by around 10 nm, which originates from the shift in the fundamental wavelength in both simulation and experiment. The pink hollow circles in figure 4 are calculated SHG intensity spectrum excited by different fundamental wavelengths from 960nm to 1060nm, which illustrates that the strongest SHG can be obtained at resonant fundamental wavelength. We also compare the measured SHG signal from the absorber with that from Au/Al_2O_3 double-layered film without Au disk on the top in experiments, the SHG generated from the absorber is enhanced by a factor of over 30.

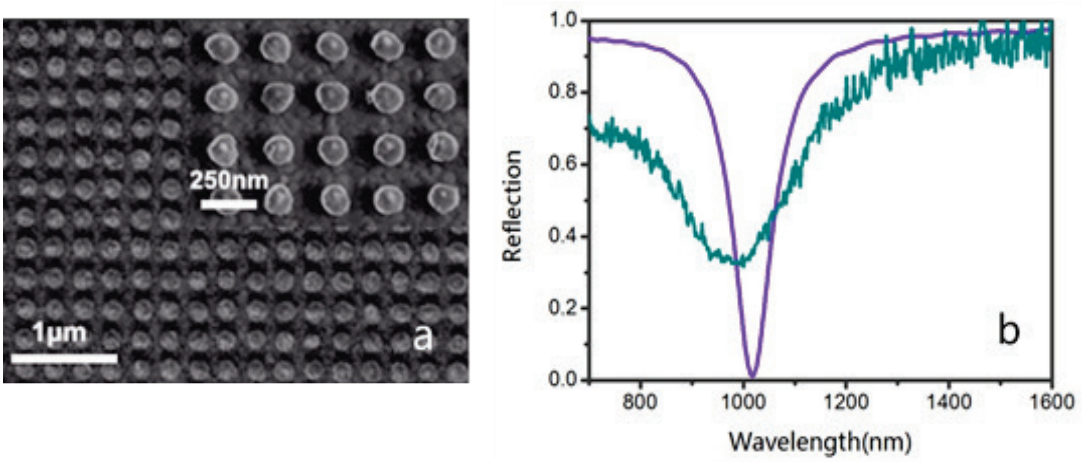

Figure 3. (a) SEM image of fabricated metamaterial absorber sample. (b) Measured (dark cyan) and simulated (purple) reflection spectra of sample with *p*=250nm, *d*=10nm and *r*=65nm.

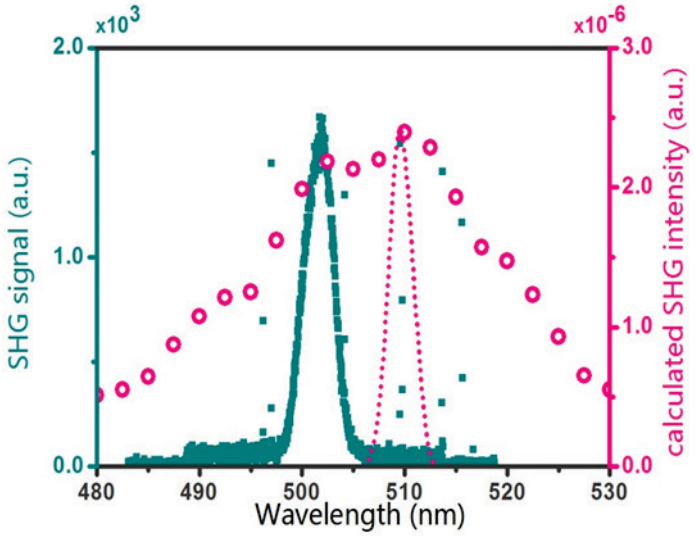

Figure 4. Measured SHG signal (dark cyan) and simulated SHG intensity (pink dot line) spectra of the sample with p=250nm, d=10nm at r=65nm, at their respective fundamental resonant wavelength of incidence. Simulated SHG intensity spectrum (pink hollow circle) of the sample with different fundamental wavelengths from 960nm to 1060nm.

4. Conclusion

We have demonstrated an Au/Al_2O_3/Au metamaterial absorber can be used for SHG enhancement. The absorbers exhibit high absorption efficiency at the dip and notably enhance the generated second harmonic signal by a factor of over 30, in contrast to an Au/alumina double-layer without Au disk on the top. This study demonstrates the potential of metamaterial absorber for nonlinear photonics.

Acknowledgment

This work is supported by the National Natural Science Foundation of China (Grant Nos. 61235007, 61425023, 61575177, 61205030 and 61275030).

References

[1] Boyd R W 2008 *Nonlinear Optics* (Amsterdam: Elsevier)
[2] Franken P A, Hill A E, Peters C W and Weinreich G 1961 *Phys. Rev. Lett.* **7** 118-119
[3] Bloembergen N, Chang R K, Jha S S and Lee C H 1968 *Phys. Rev.* **174** 813–822
[4] Sipe J E, So V C Y, Fukui M and Stegeman G I 1980 *Phys. Rev.* B **21** 4389–4402
[5] Sionnest P G and Shen Y R 1988 *Phys. Rev.* B **38** 7985–7989
[6] Scalora M, Vincenti M A, Ceglia D, Roppo V, Centini M, Akozbek N and Bloemer M J 2010 *Phys. Rev.* A **82** 043828
[7] Wang F X, Rodríguez F J, Albers W M, Ahorinta R, Sipe J E and Kauranen M 2009 *Phys. Rev.* B **80** 233402
[8] Van-Nieuwstadt J A H, Sandtke M, Harmsen R H, Segerink F B, Prangsma J C, Enoch S and Kuipers L 2006 *Phys. Rev. Lett.* **97** 146102
[9] Kim E, Wang F, Wu W, Yu Z and Shen Y R 2008 *Phys. Rev.* B **78** 113102
[10] Lesufflr A, Kumar L and Gordon R 2006 *Appl. Phys. Lett.* **88** 261104
[11] Wang B L, Wang R, Liu R J, Lu X H, Zhao J M and Li Z Y 2013 *Scientific Reports* **3** 2358
[12] Salomon A, Zielinski M, Kolkowski R, Zyss J and Prior Y 2013 *J. Phys. Chem.* C **117** 22377 −22382
[13] Rodrigo S G, Laliena V and Moreno L M 2015 *J. Opt. Soc. Am.* B **32** 15-25
[14] Thyagarajan K, Butet J and Martin O J F 2013 *Nano Lett.* **13** 1847-1851

[15] Walsh G F and Negro L D 2013 *Nano Lett.* **13** 3111 −3117
[16] Czaplicki R, Makitalo J, Siikanen R, Husu H, Lehtolahti J, Kuittinen M and Kauranen M 2015 *Nano Lett.* **15** 530-534
[17] Nahata A, Linke R A, Ishi T and Ohashi K 2003 *Opt. Lett.* **28** 423–425
[18] Kim S, Jin J, Kim Y J, Park I Y, Kim Y and Kim S W 2008 *Nature* **453** 757–760
[19] Lehr D, Reinhold J, Thiele I, Hartung H, Dietrich K, Menzel C, Pertsch T, Kley E B and Tunnermann A 2015 *Nano Lett.* **15** 1025 −1030
[20] Grinblat G, Rahmani M, Cortes E, Caldarola M, Comedi D, Maier S A and Bragas A V 2014 *Nano Lett.* **14** 6660-6665